Eddy-currents and the Force Analysis for the Thermal Shields of the MICE Spectrometer Solenoids

H. Pan[1], S. O. Prestemon[1], S. Virostek[1], R. Preece[2] and M. A. Green[1]

***Abstract*—The MICE spectrometer solenoids contain five superconducting solenoids with different structural parameters. Two coils are each separately powered. The other three coils are connected in series. The five coils are wound on a single 6061-aluminum mandrel. If one of the coils quenches, the quench will propagate by quench-back and cause other coils quench sequentially. The decaying field will induce a significant eddy current and Lorentz force on the surrounding shields. Shield eddy current heating is non-issue for the spectrometer solenoids, but the Lorentz force becomes an important aspect for designing because the five coils are not symmetric. In this paper, the detailed eddy current simulations were performed. The net lateral forces on each part of shields and the stress distribution were analyzed. Based on the Finite-element analysis, adding cuts on shields is an effective way to avoid the collapse of the shield due to changing current path direction. The shield cuts layout is presented in detail.**

***Index Terms*—Eddy current, force, quench, superconducting magnets, shields, transient stress.**

I. Introduction

THE OBJECTIVE of the Muon Ionization Cooling Experiment (MICE) is to demonstrate the designing and engineering on a section of cooling channel capable of giving the desired performance for a Neutrino Factory [1]. Two spectrometer solenoids in the MICE cooling channel will provide a uniform magnetic field for five plane scintillating fiber trackers to analyze the changing of the muon beam emittance in the cooling channel [2]. Each of the spectrometer magnet consists of five solenoids wound on a 2543 mm long 6061 aluminum mandrel as represented in Fig.1 (not drawn to scale). The center and end coils are the tracker section of the spectrometer solenoids, providing a uniform magnetic field (0.3 percent) over a length of 1000 mm and in a diameter of 300 mm; The two match coils are to match the muon beam from the Absorber Focus Coil module (AFC) into the tracker section [3,4].

All the coils are bath-cooled in liquid helium and use cryocoolers to re-condense helium vapor. In order to reduce the heat load to the cold mass, a set of shields cooled by the first stages of cryocoolers were adopted to intercept most of the radiation heat from the room temperature. The main structure of shields consist of two 9.5 mm thick neck copper shields and a 6.35 mm thick main aluminum shields including main cylinder, endplates and inner bore. Based on the previous test results, the main shields are expected to use 1100 aluminum to enhance the thermal uniformity [5].

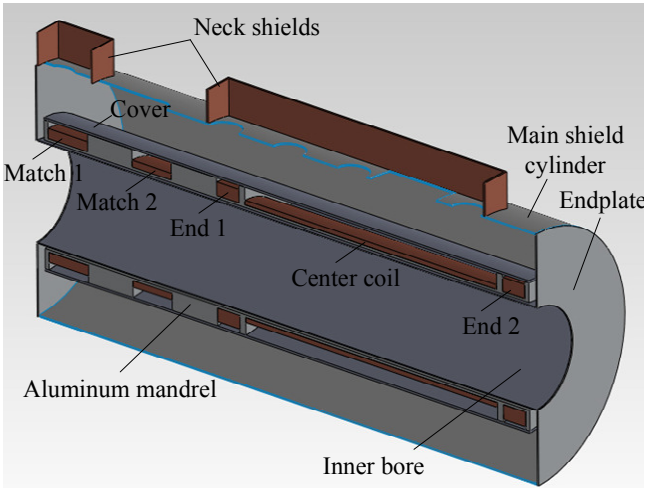

Fig. 1. The cold mass and shields cross section of the spectrometer solenoids

Because of the asymmetric structure of the cold mass, the interaction of its local magnetic field with the eddy current induced on the conductive components of the cryostat during a quench could introduce a significant lateral force on the mandrel and the shields. However, the eddy current rarely affects the mechanical stability in mandrel due to a low electrical conductivity of 6061 aluminum alloy; On the contrary, a big concern on the shields with low electrical resistance arises because a large lateral force is expected during a quench. It is necessary to assess the eddy current impact for the redesigning of the shields.

II. MICE Spectrometer Solenoids Parameters

The Spectrometer solenoid consists of five coils wound on the slotted aluminum 6061 bobbin, and covered by Al bandage wound on top of each coil to avoid separation between coil and mandrel. Table I represents the parameters of coils for this study.

TABLE I
Design Parameters for Coils

Parameter	M1	M2	E1	C	E2
No. turns/layer	120	119	66	784	62
No. layers	42	28	56	20	66
Inner radius (mm)	258	258	258	258	258
Outer radius (mm)	303	288	318	279	324
Axial coil build (mm)	201	199	111	1314	111
Initial current (A)	270	270	270	270	270

Manuscript received October 9, 2012. This work was supported in part by the U.S. Department of Energy under contract DE-AC02-05CH11231.

H. Pan, S. O. Prestemon, S. Virostek and M. A. Green are with Lawrence Berkeley National Laboratory, Berkeley, CA, 94720 USA (phone: 510-612-7137; e-mail: hengpan@lbl.gov).

R. Preece is with Rutherford Appleton Laboratory, Didcot, OX11 0QX UK. (e-mail: Roy.Preece@stfc.ac.uk).

All the coils are powered by three power supplies. The center coil, end 1 and end 2 coils are connected electrically in series using a single 300 A power supply. M1 and M2 coils will be powered by their own power supplies. Each coil has back-to-back diodes and shunt resistors. To avoid large internal voltage, the center coil is separated equally into two sectins in radial direction.

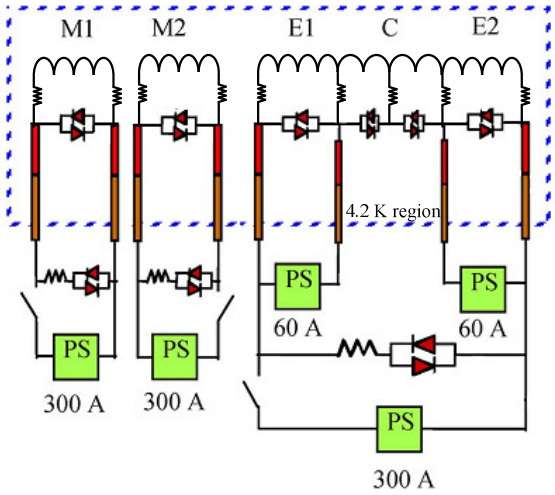

Fig. 2. General circuit diagram for spectrometer solenoids

To quantify the lateral force and optimize the shields structure, three cases of different shields designing were carried out by employing the QUENCH code of the Vector Fields OPERA 3D software. This code includes transient magnetic field analysis (ELEKTRA) coupled with thermal module (TEMPO) [6]. At each time step, it initially calculates the transient magnetic field and deduces the induced eddy currents in the mandrel and shields. The heat generation due to eddy current is calculated by using the results of previous time step and the result is processed in TEMPO module. A half 3D model including the five coils, mandrel, shields and air region was created to fulfill the simulations. When it comes to the force induced by eddy current, the worst scenario would be quench starts at the M1 coil, and then sequentially spreads to the other coils with quench-back, since the forces in different parts of shields are hard to be cancelled with each other because the field changing happens sequentially along the cold mass.

The three cases are: Case I is about all the main shields are 1100 aluminum without any electrical cuts; Case II is about 1100 aluminum shields with several cuts on both endplates and a through gap on the bottom of main cylinder; Case III is "combined" shields that utilizes 6061 aluminum inner bore and the rest parts remain the same as case II. There are some assumptions on the simulations: (1). the model is adiabatic, there is no coolant surrounding magnets assembly. (2). Neglect the insulations between coils and mandrel; (3). Assume that the initial temperature is uniform. (4). the shields temperature is uniformly 64 K at the beginning of quench.

III. Eddy Current Analysis

During a quench, the average eddy current id induced by the local flux changing on each part of shields, it can be determined by the following expression:

$$I_e = \frac{M}{R}\frac{dI_i}{dt}. \quad (1)$$

I_e is eddy current in shield; M is mutual inductance between the shield parts and each coil; I_i is transient current in coil i, R is the average resistance of the shield part. The lateral body force on shield part is:

$$F = I_e \times B_r \cdot V \quad (2)$$

B_r is the local field. V is the volume of this part. These two equations will be solved within each finite element at each time step. Ahead of the simulation, one should specify the disturbance heat to trigger a quench. In this study, a film heater was put on M1 coil, and then a quench will propagate to the other end over several seconds. Fig.3 represents the transient current in each coil in this scenario. For all the cases in this study, the local fields changing is same, however, the eddy current flow path or density is different between the cases.

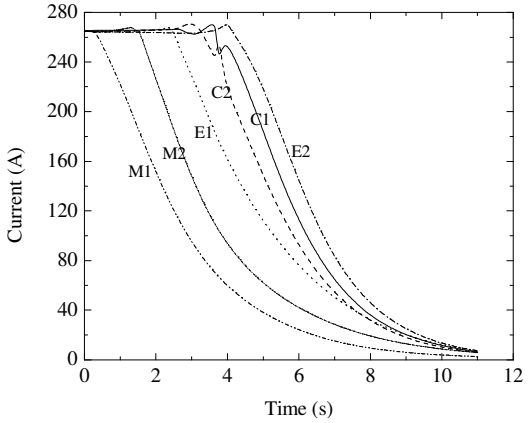

Fig. 3. Current decay in the quench initiated in M1 coil

A. Case I

Originally, the main shield cylinder is an integrated piece of 1100 aluminum without any electrical breaks. The average resistivity of 1100 aluminum is about 30 nΩ·m at 64 K. With this configuration, the main shields have a unique circle eddy-current flow path in circumference direction. The peak current density moved along the shields, and followed the quench propagation in the cold mass.

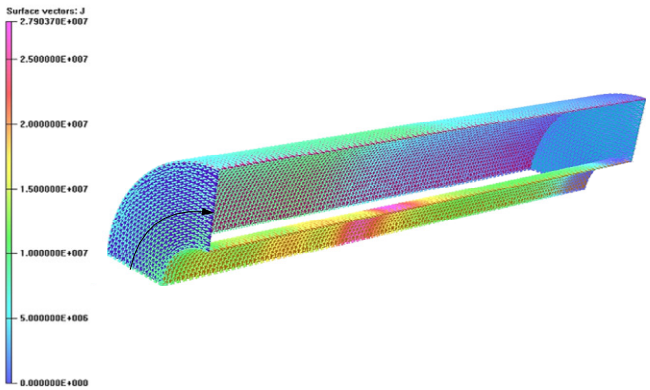

Fig. 4. Distribution of eddy current in shields at 4s since quench starts (without showing the neck shields).

Based on Fig. 3, E1 has the largest current changing at 4s since quench starts. Correspondingly in Fig.4, the peak current density is right under E1 coil. The eddy current flows clockwise through the whole shields.

From Fig. 5 it should be noted that each part of shields reached their peak value sequentially due to the quench propagation from M1 to E2. The forces in neck shields are so small that can be neglected. Because of the asymmetric fields against the mid-plane and non-uniform distribution of eddy current in shields, the net lateral force could be 160 kN, in which the forces in the outer cylinder and inner bore cylinder take a greater weight. The forces are not acceptable for shell structure that can cause a large deformation.

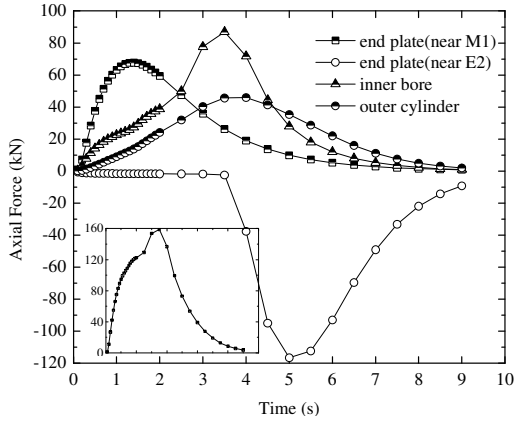

Fig. 5. Lateral forces on each part of shields, the overall lateral force on shields in small window.

B. *Case II*

From the results of case I, though the shields have met the thermal requirement of modification [5], the force is too large to keep the system stable. Case II designed a set of electrical cuts to lower the forces in each part of shields. The idea is to change eddy current path, thereby cancel same amounts of forces in shields.

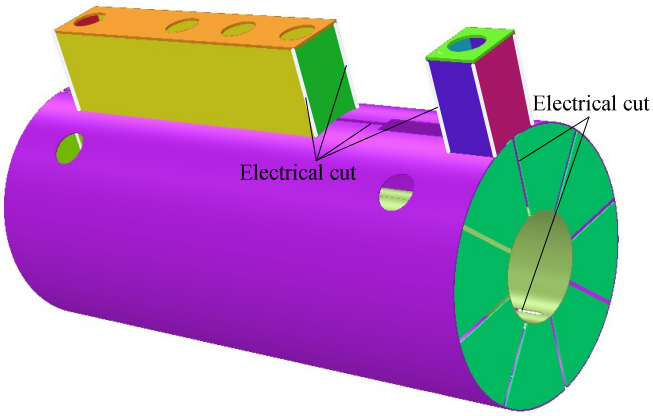

Fig. 6 Simulation model of case II

As shown in Fig. 6, a series of electrical cuts were applied: two through horizontal slits on both top and bottom on the outer cylinder has; eight radial through slits evenly distributed on each endplate, and discontinuous cut on inner bore. Meanwhile, the material of each part remains unchanged,

The eddy-current flow path is more complicated than that in case I due to the electrical cuts as represented in Fig. 7. The eddy current density concentrates on the small connections of inner bore, and it is very low in the rest parts. Compared with case I, the complicated current flows induce forces in different directions, most of which can be cancelled with each other. The outer cylinder is a good example: the current flow path forms a whole circle on the half outer cylinder; thereby the induced Lorentz forces close to two ends are in opposite directions and can be balanced.

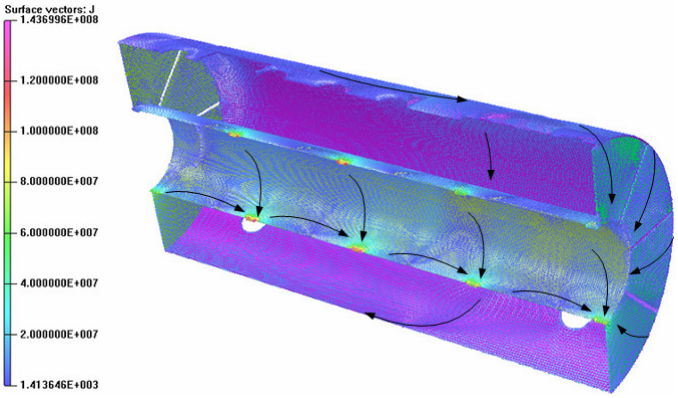

Fig. 7 Eddy current distribution in case II at 4s

Fig. 8 shows the reduced forces in each part of shields. The forces in each part reduce by 80%~90% compared with the results in case I. The peak lateral force is about 34 kN, the major part is the force in inner bore of 18 kN.

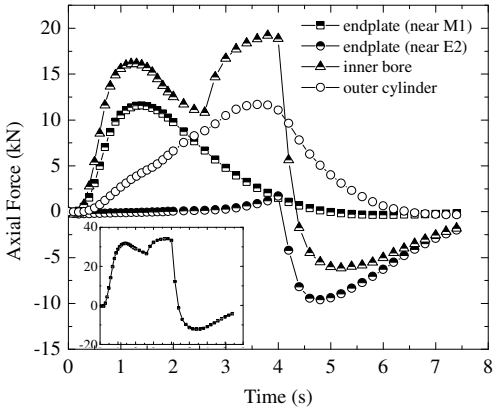

Fig. 8 Lateral forces on each part of shields, the overall lateral force on shields in small window.

The inner bore is only consternated in axial direction just by the welding line with the endplates. The force in inner bore is still needed to be lowered to reduce the deformation and local stress close to the welding line with endplates.

C. *Case III*

In case III, the inner bore was replaced to 6061 aluminum alloy to enhance the local strength, the electrical cuts remain the same as case II meanwhile.

6061 aluminum alloy has 3~4 times larger electrical resistivity than 1100 aluminum. That means the eddy current density could be much lower in 6061 Al. As shown in Fig. 9, the peak force in inner bore is about 6 kN, which is 3 factor lower than that in case II. The peak value of the overall lateral force is 19 kN.

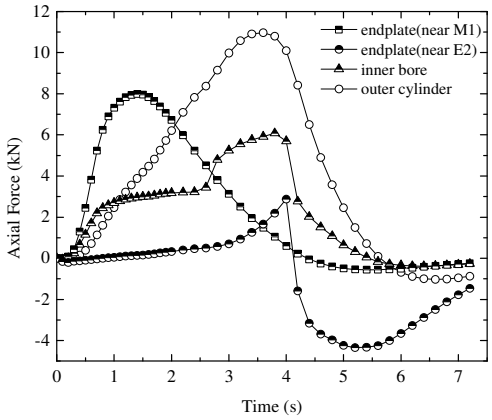

Fig. 9 Lateral forces on each part of shields.

IV. Transient Stresses Distribution in Shields

The shields are supported by four rods connected with the outer cylinder and vacuum vessel. When a lateral force applied onto the shields, the inner bore could have the largest displacement. The stress in the inner bore and endplate must be managed within the allowable range. To quantify this issue, a symmetric ANSYS model is used to simulate the stresses distribution under the peak load of case III.

In the ANSYS model, fixed displacement constraints are applied on each support; the symmetry boundary condition is applied on each face located in mid-plane. The external load is the force vector from the Vector Field model at the point of 4s after quench starts.

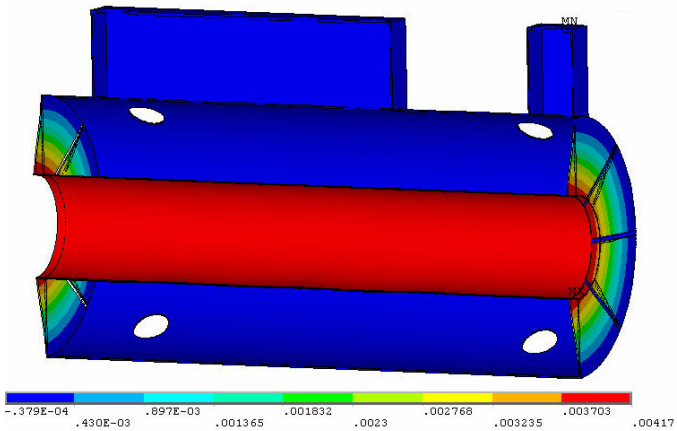

Fig. 10 Axial displacement of whole shields with a zoom scale of 10

The axial deformation of the whole shields is about 4.17 mm in inner bore (Fig. 10). Because all the shields will be wrapped layers of MLI blankets, this deformation should be restricted by putting small pieces G10 rod on vacuum vessel in axial direction.

From Fig. 11, the high stress region is the small connection of discontinuous gaps in inner bore. The peak value is about 120 MPa, which is acceptable for 6061 aluminum alloy in low temperature [7]. The peak Von Mises stress in endplates is about 65 MPa, which is lower than the allowable stress of aluminum solder. The stresses in other parts are lower than 50 MPa, which is safe for the 1100 aluminum shields.

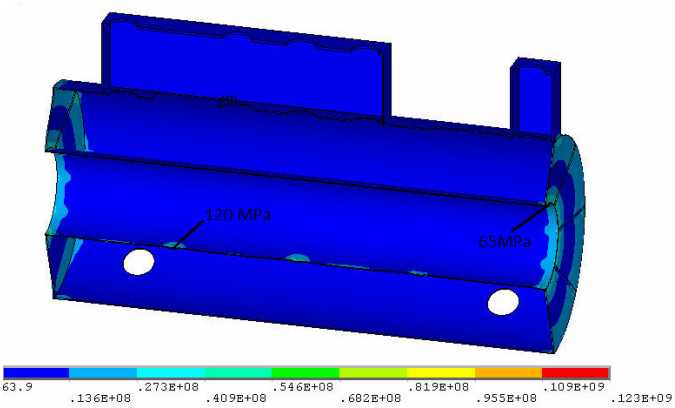

Fig. 11 Von Mises stress in the shields.

Replacing inner bore to 6061 aluminum can increase the local strength, but it also weakens the thermal performance of the shields. A thermal model with the same geometry was built to check the temperature distribution throughout the shields. Table II represents the comparison on thermal performance (the cold head is 40 K). The T_{max} in case III is acceptable for the thermal requirement (lower than the requirement of the warm end of HTS lead).

TABLE II
Temperature Difference in Case I and Case III

Parameter (K)	Case I	Case III
ΔT	7.8	13.8
T_{max}	47.8	53.8

V. Conclusion

The forces induced by eddy current in the shields for the MICE spectrometer solenoids have been analyzed and the optimization process of redesigning the shields is presented by using the 3D Vector Fields model and a ANSYS structural model. The designed electrical cutting reduces the lateral forces significantly. Replacing inner bore to 6061 aluminum provide a good compromise between stronger structure of shields against the lower thermal performance, and the combined shields is selected to finalize the shields designing.

References

[1] G. Gregoire, G. Ryckewaert, and L. Chevalier *et al.*, "MICE and international muon ionization cooling experiment technical reference document," 2001 [Online]. Available: http://www.mice.iit.edu

[2] B. Wanget al. , "The design and construction of the MICE spectrometer solenoids," IEEE Trans. Applied Superconductivity , vol. 19, no. 3, pp. 1348–1351, 2009

[3] M. A. Green, S. P. Virostek, W. W. Lau, and S. Q. Yang, "Progress on the MICE tracker solenoid," in Proceedings of EPAC-06, Edinburgh, UK, 2006 [Online]. Available: http://mice.iit.edu, MICE Note 158

[4] S. P. Virostek and M. A. Green, "The Results of Tests of the MICE Spectrometer Solenoids," IEEE Trans. Applied Superconductivity , vol. 20, no. 3, pp. 377–380, 2010.

[5] S. P. Virostek, "Spectrometer Solenoid Update," MICE Collaboration Meeting 30, Oxford University, 2011.

[6] *Vector Fields Opera-3D Reference Manual*, ERA Technol. Ltd., Surrey, U.K., 2008.

[7] J. E. Jenson, W. A. Tuttle, and R. B. Stewart *et al. Brookhaven National Laboratory Selected Cryogenic Data Notebook.* Brookhaven National Laboratory Associated University Inc., U.S., 1980.